

## Electron Capture by $\text{Ne}^{10+}$ Trapped at Very Low Energies

C. R. Vane, M. H. Prior, and Richard Marrus

*Materials and Molecular Research Division, Lawrence Berkeley Laboratory, Berkeley, California 94720, and  
Department of Physics, University of California, Berkeley, California 94720*

(Received 30 September 1980)

An electrostatic ion trap was used to trap  $\text{Ne}^{q+}$  ( $1 \leq q \leq 10$ ) ions created by a fast xenon beam passing through neon gas. Exponential decay in time of the  $\text{Ne}^{10+}$  fraction due to electron capture from neon gas was observed and the decay rates measured. For mean kinetic energies between 7–45 eV, the total electron-capture cross section ( $\sigma_{ec}$ ) is found to be velocity independent. For this energy range we obtain  $\sigma_{ec}(\text{Ne}^{10+}) = 2.4 \times 10^{-15} \text{ cm}^2$ , with an estimated uncertainty of 30%.

PACS numbers: 34.70.+e, 82.30.Fi

Electron capture by low-energy multiply charged ions on neutral gases has been a subject of considerable recent interest in connection with fusion research<sup>1</sup> and astrophysical problems.<sup>2</sup> A number of calculations have resulted, which are based on a variety of models.<sup>3</sup> Experimental progress has been achieved mainly with use of beam-gas techniques,<sup>4</sup> but for multicharged heavy ions has been almost entirely confined to the kinetic-energy range above  $\sim 1$  keV and charge states less than fully stripped. In this Letter a new technique is described that uses the low-energy multicharged recoil ions produced in a gas traversed by a fast heavy-ion beam.<sup>5</sup> These ions are held in an electrostatic trap where they undergo electron capture from the atoms in the residual gas. By sampling the ion population in time after their creation, the decay rates associated with electron capture are directly measured. Varying the trap potential allows determination of these rates as a function of ion kinetic energy. From this information, it is possible to infer values for the total cross section for electron capture and its velocity dependence. As a demonstration, a measurement of the total capture cross section of  $\text{Ne}^{10+}$  (fully stripped) on neutral neon gas in the range of mean kinetic energies 7–45 eV is described. However, the method has application to very low-energy, high-charge states of a wide variety of ions and target gases.

Pulsed 3.5-MeV/u  $\text{Xe}^{27+}$  beams from the Lawrence Berkeley Laboratory (LBL) SuperHILAC were collimated to  $\sim 1.25$  cm diameter and passed through an ultrahigh-vacuum target chamber isolated from the  $\sim 10^{-6}$ -Torr vacuum of the beam line by thin ( $\sim 150 \mu\text{g}/\text{cm}^2$ ) carbon foils. The base chamber pressure was typically  $1 \times 10^{-8}$  Torr. The mean charge state of the foil-transmitted beam, calculated with a formula given by Betz,<sup>6</sup> was  $\text{Xe}^{38+}$ . The ion beam was collected in

a Faraday cup several meters downstream of the chamber. The collected charge was used for data normalization, and a beam-arrival pulse was generated for timing synchronization. An electrostatic ion trap<sup>7</sup> was constructed as shown schematically in Fig. 1. It consists of a  $\sim 15$ -cm-diam copper cylinder  $\sim 18$  cm in length and a coaxial electrically isolated thin tungsten wire (diameter, 0.08 mm). A potential difference ( $\Delta V$ ) between these elements produced a nearly logarithmic potential well in which slow positive ions were radially confined. Isolated end caps, held at an appropriate potential with respect to the central wire, restricted ion motion parallel to the axis so that a three-dimensional trapping configuration could be achieved without seriously disturbing the logarithmic potential near the trap center. The ion trap was mounted in the target chamber so that the projectile beam was transmitted axially through the trap parallel with the central wire at a separation of 1.25 cm.

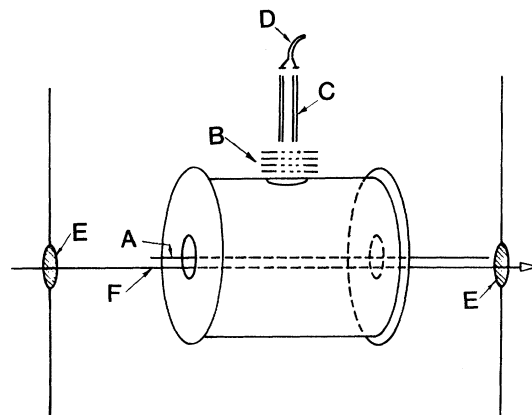


FIG. 1. Electrostatic ion trap. A, central wire; B, acceleration/deceleration grids; C, quadrupole  $m/q$  analyzer; D, channel electron multiplier; E, vacuum isolation foils; F, beam axis.

Neon target gas was admitted into the trap region from a clean glass reservoir through a variable-leak valve. The reservoir contained target gas at a pressure of a few Torr to allow smooth control of low  $[(1-6) \times 10^{10}/\text{cm}^3]$  target densities. The pressure in the trap region was measured with a nude Bayard-Alpert ion gauge calibrated for neon by comparison (over two orders of magnitude) with a capacitance manometer.

Target ions created during the 3.3-msec  $\text{Xe}^{38+}$ -beam pulse recoil at nearly  $90^\circ$  with respect to the incident beam, i.e., in a plane perpendicular to the trap axis. The recoil energies of these ions may be estimated from production cross sections obtained by extrapolation from existing measured values.<sup>5</sup> The Coulomb impulse from the fast projectile, with a  $\text{Ne}^{10+}$ -production cross section of  $\sim 10^{-17} \text{ cm}^2$ , yields a recoil energy of a few electron volts for the bare ions. Thus, trap well depths produced by potential differences of only tens of volts across the elements are greater than initial ion-recoil energies. The ion trap was insensitive to the mass or charge of the bound ion. Hence, essentially all  $\text{Ne}^{q+}$  ions formed in the trap with nonzero angular momentum about the central wire are confined and are found to have average kinetic energies which depend only upon the trap parameters.

The trapped  $\text{Ne}^{q+}$  ions interact with neutrals in the thin background gas while orbiting the central wire. Elastic and inelastic collisions can occur, but impact energies are usually too low for ionization of neutrals except through electron capture, and for the trap geometry chosen very few elastic collisions can lead to loss of the ions from the trap (only those which reduce the ion angular momentum to essentially zero). Therefore, decay of a  $\text{Ne}^{q+}$  population through interactions with neutral target gas is due primarily to electron capture collisions.

The bare-ion decay rate was measured by emptying the ion trap at progressive delay times after detection of the projectile-beam pulse and by storing the number of  $\text{Ne}^{10+}$  ions released into the detection system as a function of time. Ions were dumped from the trap by switching the central wire potential from its negative trapping value to the positive potential of the outer cylinder. A geometric fraction of the released ions passed through a grid-covered hole in the trap outer cylinder. Transmitted ions were filtered according to their mass-to-charge ratio ( $m/q$ ) by a commercial quadrupole residual-gas analyzer (RGA) and detected by a channel electron

multiplier, as shown in Fig. 1. Isotopically pure  $^{22}\text{Ne}$  target gas was used in these experiments. The RGA resolution is sufficient to separate all charge states of  $^{22}\text{Ne}^{q+}$  and, in particular, to fully resolve  $m/q = 2.20$  ( $^{22}\text{Ne}^{10+}$ ) ions from  $m/q = 2.00$  ions (e.g.,  $\text{H}_2^+$ ). The RGA can be remotely scanned at fixed delay times to provide  $m/q$  spectra for calibration and to ensure negligible background signal from other gases. To preclude the possibility of substantial levels of contaminants being introduced with the target gas,  $m/q$  scans were taken at widely varied target densities and the spectra searched for pressure-dependent non- $^{22}\text{Ne}^{q+}$  peaks. None were found.

In measurements of the decay rates of  $\text{Ne}^{10+}$ , the RGA was programmed to transmit only  $m/q = 2.20$  ions. The time interval from production to release of the ions from the trap (trapping time  $t_i$ ) was then scanned in a stepwise fashion, remaining at each value  $t_i$  for many beam pulses until a prescribed beam charge accumulated at the Faraday cup. The trapping time was then incremented and the process repeated until the period between beam pulses had been scanned. The ion counts were stored by a minicomputer in multichannel scaling mode, each channel corresponding to a particular  $t_i$ .

The resulting decay curves are well described by a single exponential,  $N = N_0 e^{-\gamma t}$ , as shown by the semilog plots of Fig. 2. The decay rate,  $\gamma$ , can be expressed as  $\gamma = \langle \sigma v \rangle n + \gamma_0$ , where  $\gamma_0$  is the net decay rate associated with trap leakage and collisions with background gases other than

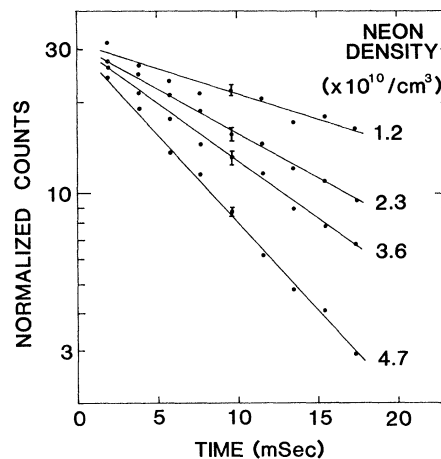


FIG. 2. Decay of trapped  $\text{Ne}^{10+}$  at trap potential of 20.7 V for various neon densities. Each curve has been normalized at  $t = 0$ , corresponding to the trailing edge of the beam pulse. Error bars indicate statistical uncertainties of the data.

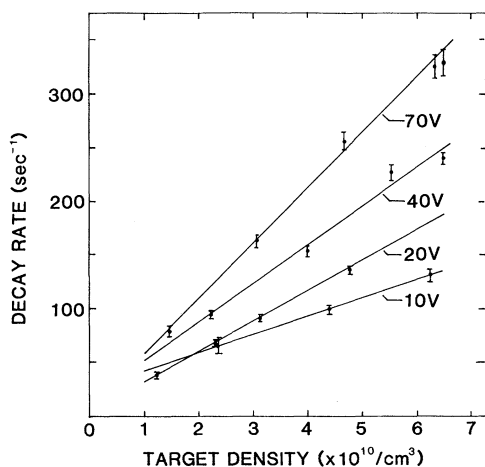


FIG. 3.  $\text{Ne}^{10+}$  decay rates as a function of target density for trap potentials shown. Slopes give  $\langle\sigma v\rangle$  for electron capture from neon.

neon;  $\langle\sigma v\rangle n$  is the decay rate of  $^{22}\text{Ne}^{10+}$  due to electron capture to all lower-charge states from neutral  $^{22}\text{Ne}$  at density  $n$ . The rates  $\gamma$  vs  $n$  were obtained from least-squares fits to series of data such as those shown in Fig. 2. Plots of  $\gamma$  vs  $n$  for several trap potentials are shown in Fig. 3. The slopes of straight-line fits to these data provide  $\langle\sigma v\rangle$ , the capture collision rate constant averaged over the  $\text{Ne}^{10+}$  velocities at each trap potential. The extrapolated decay rate for  $\text{Ne}^{10+}$  ions at zero neon density was approximately  $3 \text{ sec}^{-1}$ , consistent with ion loss due to electron capture from the  $\text{N}_2$ - and  $\text{H}_2\text{O}$ -dominated background density of about  $6 \times 10^8 \text{ cm}^{-3}$ .

By switching off the trap in a time significantly shorter than a trapped-ion "orbital" period (greater than several microseconds), the  $\text{Ne}^{10+}$  are released unperturbed. This "fast-dump" technique was employed in time-of-flight (TOF) and retardation measurements (with use of the acceleration/deceleration grids shown in Fig. 1) to study the velocity distribution of  $\text{Ne}^{10+}$  ions in the trap. The results are consistent with ion motion calculated in a model assuming a purely logarithmic radial potential, which was not unexpected, as the ions observed are restricted to those near mid-length of the trap. TOF data were acquired at several trapping times in an attempt to observe time evolution of the velocity and spatial distributions of the bound ions. No significant variation was observed, strong evidence that loss of  $\text{Ne}^{10+}$  by mechanisms other than electron capture is negligible.

The virial theorem applied to ion motion in the

TABLE I. Variation of capture rate constant  $\langle\sigma v\rangle$  with trap potential  $\Delta V$ .

$\Delta V$ (V)	$v_{\text{rms}}$ ( $10^6 \text{ cm/sec}$ )	$\langle\sigma v\rangle$ ( $10^{-9} \text{ cm}^3/\text{sec}$ )
70.7	2.02	$5.1 \pm 0.2$
40.7	1.53	$3.6 \pm 0.3$
20.7	1.09	$2.8 \pm 0.1$
10.0	0.76	$1.7 \pm 0.1$

plane perpendicular to the trap axis near trap mid-length shows that the rms ion velocity ( $v_{\text{rms}}$ ) is independent of initial conditions and depends only on the trapping potential as  $v_{\text{rms}} = C(q \Delta V)^{1/2}$ , where  $C = 7.6 \times 10^4 \text{ cm/sec} \cdot \text{eV}^{1/2}$  is determined by the geometry of the trap and ion mass. This has been compared with the mean ion velocities from the TOF and retardation data, and found to be consistent with those results to within 10%. Table I contains the  $\text{Ne}^{10+}$ -capture rate constants determined at several trap potentials. Under the assumption of a power-law dependence  $\langle\sigma v\rangle = A(q \Delta V)^p$ , a least-squares fit to the data yields  $p = 0.54 \pm 0.05$ . Figure 4 demonstrates the constancy of  $\langle\sigma v\rangle / (\Delta V)^{1/2}$  with  $(\Delta V)^{1/2}$ , implying that in the range of impact energies studied here, the cross section is velocity independent. A forced fit of  $\langle\sigma v\rangle = \sigma_{ec} v_{\text{rms}}$  to the data yields  $\sigma_{ec} = [2.4 (\pm 0.2)] \times 10^{-15} \text{ cm}^2$ . This error is the statistical error in the least-squares fit. The absolute error is estimated to be 30%, primarily from uncertainty in the neon density.

A simple semiclassical model to describe the electron-capture process in the low-energy re-

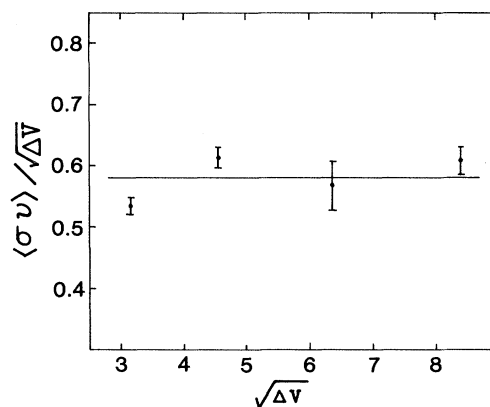


FIG. 4. Decay rate constant  $\langle\sigma v\rangle$  scaled by  $(\Delta V)^{-1/2}$  vs  $(\Delta V)^{1/2}$ . Units of vertical and horizontal axes are  $10^{-9} \text{ cm}^3/\text{sec} \cdot \text{V}^{1/2}$  and  $\text{V}^{1/2}$ , respectively. Error bars indicate only the statistical errors in least-squares fits to the data.

gime has recently been proposed.<sup>8</sup> A prediction of this model is that charge capture ends up with high- $n$  states, where  $n$  is determined by two conditions. First, the energy of the level into which the electron is captured must be equal to the perturbed binding energy in the target atom. Second, the target and projectile must approach sufficiently close so that electron transfer is classically possible. Studies conducted at Gesellschaft für Schwerionenforschung, Darmstadt,<sup>9</sup> are in good agreement with the predicted states. A further prediction of the model is that the cross sections are velocity independent. Our value for the total cross section is in agreement with the semiclassical result,  $\sigma_{sc} = 2.5 \times 10^{-15} \text{ cm}^2$ , for one-electron capture into  $n \approx 5$ .

We acknowledge the invaluable assistance of Dr. Harvey Gould, Mr. Douglas MacDonald, and the operators and staff of the LBL SuperHILAC. This work was supported by the Fundamental Interactions Branch, Division of Chemical Sciences, Office of Basic Energy Sciences, U. S. Department of Energy, under Contract No. W-7405-Eng-48.

---

<sup>1</sup>H. B. Gilbody, in *Advances in Atomic and Molecular Physics*, edited by D. R. Bates (Academic, New York, 1979), Vol. 15, p. 293.

<sup>2</sup>A. Dalgarno, in *Advances in Atomic and Molecular Physics*, edited by D. R. Bates (Academic, New York, 1979), Vol. 15, p. 37.

<sup>3</sup>For a summary of many relevant references, see R. E. Olson, in *Electronic and Atomic Collisions*, edited by N. Oda and K. Takayanagi (North-Holland, Amsterdam, 1980), p. 391.

<sup>4</sup>D. H. Crandall, R. A. Phaneuf, and F. W. Meyer, *Phys. Rev. A* **22**, 379 (1980), and references therein; E. Salzborn and A. Muller, in *Electronic and Atomic Collisions*, edited by N. Oda and K. Takayanagi (North-Holland, Amsterdam, 1980), p. 407.

<sup>5</sup>I. A. Sellin *et al.*, *Z. Phys. A* **283**, 320 (1977); C. L. Cocke, *Phys. Rev. A* **20**, 749 (1979); T. J. Gray, C. L. Cocke, and E. Justiniano, *Phys. Rev. A* **22**, 849 (1980); H. F. Beyer *et al.*, in *Proceedings of the Eleventh International Conference on the Physics of Electronic and Atomic Collisions*, edited by N. Oda and K. Takayanagi (Society for Atomic Collision Research, Japan, 1979), p. 602.

<sup>6</sup>H.-D. Betz, *Rev. Mod. Phys.* **44**, 465 (1972), p. 512; see Eq. (5.7), in particular.

<sup>7</sup>K. H. Kingdon, *Phys. Rev.* **21**, 408 (1923). Ion trajectories in the logarithmic potential have been calculated by R. H. Hooverman, *J. Appl. Phys.* **34**, 3505 (1963).

<sup>8</sup>H. F. Beyer, Ph.D. thesis, Gesellschaft für Schwerionenforschung, Darmstadt, Report No. 79-6, 1979 (unpublished), ISSN:0171-4546; H. Ryufuku *et al.*, *Phys. Rev. A* **21**, 745 (1980).

<sup>9</sup>R. Mann, F. Folkmann, and H. F. Beyer, to be published.